Shock Waves (1998) 8: 1–9

Shock Waves

The puzzle of whip cracking – uncovered by a correlation of whip-tip kinematics with shock wave emission*

P. Krehl[1], **S. Engemann**[1], **D. Schwenkel**[2]

[1] Ernst-Mach-Institut, Institut für Kurzzeitdynamik der Fraunhofer-Gesellschaft, D-79104 Freiburg, Germany
[2] VKT Video Kommunikation GmbH, D-72787 Pfullingen, Germany

Received 3 March 1997 / Accepted 21 July 1997

Abstract. During whip cracking the whip-tip reaches a supersonic velocity for a period of about 1.2 ms, thereby emitting a head wave with a parabolic-shaped geometry. A detailed study of this mechanism which encompasses the motion analysis of the whip-tip as well as the determination of the local origin of the shock emission requires a sophisticated recording technique. A pre-trigger framing high-speed video camera system was used which was triggered by an acoustical sensor and synchronized with a pulsed copper-vapour laser. The phenomena were visualized by the direct shadowgraph method and recorded cinematographically as digital images at a frame rate of 9 kHz using a CCD-matrix with 256(H) $\times$ 128(V) pixels. The resulting series of frames allowed, for the first time, (i) a reconstruction of the whip-tip trajectory, (ii) a determination of the tuft velocity and acceleration, (iii) a correlation of whip-tip kinematics with shock wave emission, and (iv) a motion analysis of the turning and unfolding mechanism of the tuft. The tuft at the whip-tip was accelerated within a distance of about 45 cm from a Mach number of $M = 1$ to a maximum of $M = 2.19$, thereby reaching a maximum acceleration of 50,000 g. The shock is emitted at the moment when the cracker, arriving at the turning point of the lash, is rapidly turned around. After emission of the shock wave the tuft is strongly decelerated to $M < 1$ within a short distance of only 20 cm.

Key words: Whip cracking, Shock visualization, Head wave, High-speed videography, Pre-trigger framing cinematography

1 Introduction

Whip cracking is probably the oldest means available to man of generating shock waves. Since antiquity its sharp piercing report has been used as an aid for drovers, tamers and coachmen, and even in our times it is practiced traditionally for quite different reasons in Southern Germany and Switzerland.[1]

To provide an effective cracking, i.e. controlling the whip with a minimum of strength to get a crack as loud as possible, special whip constructions have been evolved, all based on practical experience and empiricism. In general, an "optimum whip" is incrementally assembled, each element becoming lighter and more slender towards the end of the whip. Figure 1 shows as an example a view of such a whip construction. It consists of: (1) a long elastic handle made of several braided wooden sticks; (2) two loosely connected leather straps, and (3) a tight-braided thong of two leather laces. The lash at the whip-tip is stepped and consists of hemp, or nowadays, a fine-braided cord of synthetic fibers which is tightly braided threefold to form part (4), and twofold to form part (5). The terminal lash (6) consists only of a single cord. The most important part of the whip is the so-called cracker (c) at the lash-tip, a short piece of the cord, some centimeters in length, behind the knot which is frayed out to form a brush or tuft. The knot alone cannot provide an effective cracking sound, which can easily be demonstrated by just cutting away the tuft. To further improve the cracking efficiency, some professional whip operators provide the outermost part of the lash with additional knots (k) which certainly increase the mass and, therefore, accumulate the kinetic energy at the whip-tip. The bull whip, a derivative of the East European karbatsche, has a short leathern stick. It is heavier constructed than the whip shown in Fig. 1 and can reach a length of up to 6 m.

* Paper first presented at the Spring Meeting of the *Deutsche Physikalische Gesellschaft*, Section *Kurzzeitphysik*, March 18-21, 1996, University of Rostock, Germany
Correspondence to: P. Krehl

[1] In Southern Germany whip cracking has been practiced at Shrovetide since the Middle Ages to generate noise and used besides other instruments like bells, rattles and drums to contrast the following Lent, a period of silence and contemplation. The popular conception that the rite of noise generation has pagan roots and was originally practiced in order to cast out the winter demons has not yet been proved scientifically (Mezger 1991). In Upper Bavaria *Aperschnalzen*, a distinguished kind of whip cracking is celebrated annually as a competition (Kapfhammer 1977), and was first demonstrated worldwide in 1972 at the open ceremony of the Olympic Games in Munich. – In Switzerland whip cracking is used traditionally in some alpine valleys for communication purposes and applied besides cow-bells and alp horns, while in some central areas it is practiced at St. Nicholas' Day in a particular, rhythmic manner (Mezger 1997).

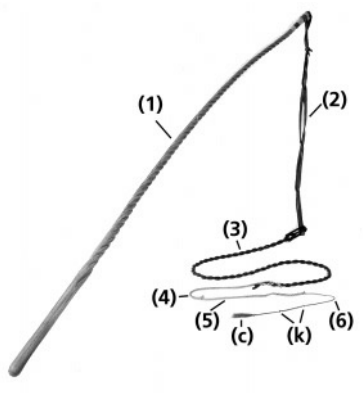

Fig. 1. View of a whip particularly constructed to generate strong cracks

In the beginning of gas dynamics, a discipline only a good century old, the mechanism of shock generation by supersonic phenomena was not understood and high-speed photography was still in its infancy. Despite these deficiencies it is surprising that the puzzle of whip cracking, a highly transient supersonic phenomenon not directly resolvable by the naked eye, was already under investigation, and one important condition, the supersonic motion of the whip-tip, was already correctly presumed. However, it will be shown here for the first time that this is not the only condition needed to generate strong shocks.

To uncover and correlate all these details of the mechanism of whip cracking, a complex fast pre-trigger framing recording system with a frame rate of at least 50 kHz and a resolving power of better than 20 lp/mm would be required. Such a system, however, is not yet commercially available. Nevertheless, using laser stroboscopy combined with state-of-the-art high-speed videography and a direct shadowgraph technique a deeper insight look into the puzzle of whip cracking was obtained, and for the first time an exact correlation between whip-tip dynamics and shock-wave emission, as well as visualization of the behavior of the cracker after entering the supersonic phase, was achieved.

The present study of whip cracking was initiated by the ZDF (*Zweites Deutsches Fernsehen*, Second German Television) which had asked for a movie to demonstrate this phenomenon in a popular-science telecast. The recording technique used for the visualization of these events of uncontrolled occurrence may be of interest for the visualization of entirely different high-speed phenomena, for example the bursting behavior of pressurized vessels, thus allowing the study of shock effects as well as their local origin and causality.

2 Historical background

In the period 1885-1887 Ernst Mach and Peter Salcher carried out their famous supersonic ballistics experiments which showed that a projectile moving with a velocity exceeding the sound velocity generates a characteristic cone-shaped shock wave, the so-called head wave.[2] In general, any body moving with supersonic velocity produces such head waves, and Mach and Doss (1899) assumed that the sharp bang of a meteorite approaching the earth and entering the atmosphere with supersonic velocity is created by a head wave. Lummer (1905), Fig. 2, was the first who, inspired by Mach's publications, explained whip cracking by the head wave phenomenon. He correctly assumed that the sharp report is caused by the free end of the whip which eventually reaches supersonic speed. Although Lummer was derided by his friends and colleagues for this interpretation, Winkelmann (1909) and Prandtl (1913) acknowledged his hypothesis in their encyclopedic articles, and from thereon it became common knowledge in many textbooks on acoustics and gas dynamics. However, a definite experimental proof had yet to come.

Fig. 2. Portrait of Otto Lummer (1860–1925), professor of physics at Breslau University who as early as 1905 speculated on whip cracking as being a supersonic phenomenon (Courtesy of *Deutsches Museum München*)

Lummer also tried to approach the problem experimentally. Unfortunately, his cinematographic technique could not resolve the dynamics of the whip-tip in its final stage of acceleration, the essential phase in the process of whip cracking. His studies could only resolve the middle part of the lash which revealed a maximum velocity of only 200

[2] The expressions "head wave" (*Kopfwelle*) and "tail wave" (*Achterwelle*) were coined by E. Mach (1887) and introduced into the English literature by C.V. Boys (1893). Both waves can have slightly different cone angles. In the case of whip cracking the moving body, i.e. the cracker, is quite small and both waves practically merge into each other.

m/s. The first progress in the experimental confirmation of Lummer's hypothesis was made by Carrière (1927, 1953) in France at the Institut Catholique de Toulouse. To facilitate the visualization of the whip-tip dynamics within a fixed field of view and at a constant depth of focus, he constructed a machine-driven whip. Using a multiple spark chronograph he observed that the whip-tip could reach a maximum velocity of 900 m/s (Carrière 1953). Furthermore, in a cumbersome series of experiments he even obtained the first still shadowgraphs of the emitted shock wave. However, instead of a head wave characterized by a parabolic-shaped or a conical shock front, he observed a circular wave structure fully surrounding the whip-tip.

Lummer's hypothesis was first theoretically supported by Grammel and Zoller (1949) from the University of Stuttgart. Their research was initiated by the eye-clinic at the University of Göttingen where strange eye injuries had been diagnosed. Small pieces of copper wire had deeply penetrated into the eye, but barely left an injury to the cornea. These patients were coachmen who had used whip lashes of stranded copper wire instead of textile or leather materials. This raised the question whether these micro projectiles were originated during whip cracking and how supersonic processes were involved. Grammel and Zoller proved mathematically that at increasing time during propagation of the lash loop towards the free end the velocity of the whip-tip could increase without limit.

The experimental results of Carrière were later extended for a real whip by Bernstein, Hall and Trent (1958) at the U.S. Naval Research Laboratory. They used a bull whip which was operated by an expert whip cracker. Using a movie camera at 120 frames/sec they clearly resolved the lash dynamics, particularly the formation of the loop in the lash which propagates towards its tip, thereby quickly increasing in speed and finally exceeding the sound velocity when approaching the whip-tip. This last phase occurs in the submillisecond regime and was resolved using a high-speed camera at a frame rate of 4 kHz. The evolution of shock waves was visualized by a still camera, and the resulting snapshots, taken at various time instants and pseudo-cinematographically composed, clearly revealed for the first time the typical head wave character of the emitted crack. Later these results, originally published in an acoustical journal and barely noticed among the shock physics community, became better known by the excellent booklet of Glass (1974) on cosmic, terrestrial and man-made shock-wave phenomena.

Bernstein et al. also extended the mathematical model of Grammel and Zoller and calculated the tension in the lash which increases without limit as the traveling loop approaches the tip. Similar results were also obtained by Szabó (1972, 1976), professor of mechanical engineering at the Technical University Berlin. Being a Hungarian by birth, he used to demonstrate in his lectures whip cracking with a Hungarian pastoral whip, a sort of bull whip. He approached the problem mathematically from the viewpoint of classical mechanics rather than from gas dynamics and came to the same conclusion that the tip can move faster than the sound velocity.

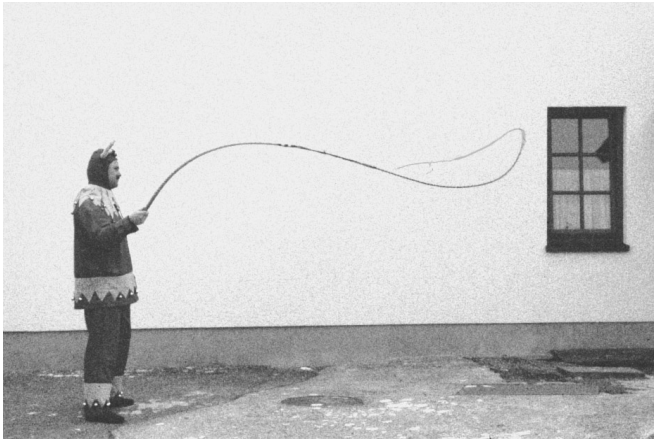

Fig. 3. Black Forest whip cracker at Shrovetide showing whip cracking in its final phase and shortly before shock emission. Note the loop which, starting from the whip-stick and traveling down the lash, has almost reached the whip-tip

3 Schematics of whip lash dynamics

In order to produce a sharp cracking sound, it is necessary to throw the lash in such a way that it starts as a sharp loop near the handle. This initial phase starts rather slowly and in the very beginning can even be resolved by the trained eye. Figure 3 shows the position of the loop just before arriving at the lash end.

Theoretically, the phenomenon of whip cracking can be explained by the dynamic behavior of a buckling discontinuity in a rope. When a rope with a free end is pulled at constant translation velocity around a sharp bend of small radius, the free end is accelerated by the centrifugal force to a higher velocity than the translation velocity (Kucharski 1941). This effect increases with decreasing length of the free end and can lead to a very high velocity of the free end. The same mechanism also happens at whip cracking with the only difference that the loop itself travels down the lash towards the tip, while the whip-stick, and therefore the lash between the stick and propagating loop, remain almost at rest. Since the kinetic energy stored in the moving lash is focused into an increasingly shorter and lighter piece of the remaining whip-lash, the law of conservation of energy requires that the velocity of the free end strongly increases when it approaches the lash-tip.

This phenomenon of the traveling loop is important in order to understand the development of the supersonic phase and is depicted schematically in Fig. 4. Recently, Bürger (1995) demonstrated that in a suitable frame of reference the spatial velocity of the whip-tip $V(x)$ can be calculated simply by applying the law of conservation of energy. He presumed (1) an infinitesimal bend radius $r \to 0$, (2) a whip-stick at rest, and (3) neglected any air drag effects. At the beginning, Fig. 4a, the whole lash is straight and moves with the velocity U from right to left. For a lash of length L and mass M with an attached cracker of mass m, the law of conservation of energy requires that

$$\frac{1}{2}(M+m)U^2 = \frac{1}{2}\left(M\frac{L+x}{2L}+m\right)V^2$$

which yields for the velocity of the lash-tip

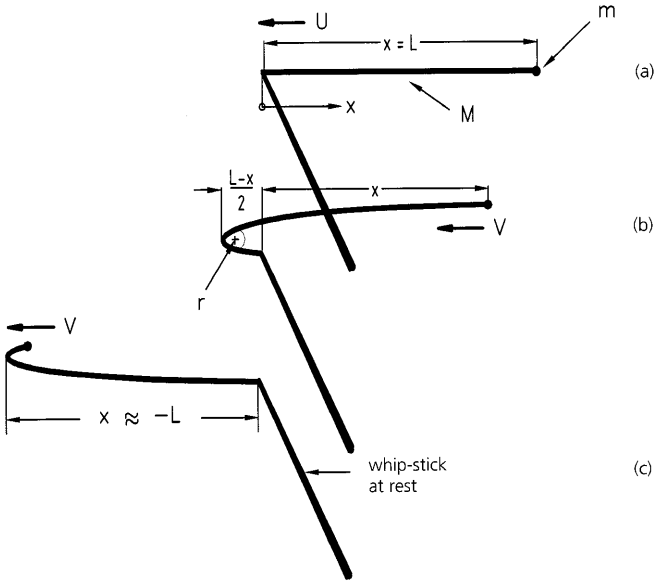

Fig. 4. Simple model of whip-loop motion after Bürger (1995): **a** starting position with lash at velocity U, propagating from left to right; **b** intermediate position; and **c** briefly before reaching maximum whip-tip velocity

$$V(x) = U\frac{\sqrt{\frac{M}{m}+1}}{\sqrt{\frac{M}{m}\,\frac{L+x}{2L}+1}}\,.$$

At the beginning the cracker is positioned at $x = +L$, and the whip-tip has the same translation velocity as the lash, i.e. $V = U$. However, with increasing propagation in the x-direction $V(x)$ grows and, approaching the free end at $x \to -L$, reaches the maximum velocity

$$V_{\max} = U\sqrt{\frac{M}{m}+1}$$

which increases without limit for an infinitesimal cracker mass ($m \to 0$). For a stepped whip-lash construction such as shown in Fig. 1, the ratio M/m is quite high and reaches a value of almost 300. Although in practice the assumptions (1)–(3) are not fulfilled as will be shown below, the simple model clearly demonstrates that V can reach at least an order of magnitude greater than U.

Assumption (2) requires that the lash moves in an inertial system with the stick at rest at all times, i.e. that the hand does not perform any work. However, to further increase the shock intensity it is a common practice of whip experts to pull the stick with a jerk in the positive x-direction when the loop is still in the intermediate state, as illustrated in Figs. 3 and 4b. This might increase the velocity V when reaching the turning point and intensify the Kucharski effect. The present measurements, however, could not demonstrate this effect, because only the final state of the loop was observed, as shown in Fig. 4c, and the stock was far beyond the field of view.

4 Experimental arrangement

4.1 Problems of shock visualization

Contrary to the initial phase of whip cracking the recording of the supersonic phase provides various technical problems. It is impossible even for an expert whip cracker to operate the whip-tip in such a way that (1) his movements and body heat do not disturb the flow in the field of view, and the crack is (2) generated reproducible at a fixed location and (3) triggered precisely at a given time instant.

Problem (1) excludes the application of highly-sensitive optical methods for recording the shock such as schlieren or interferometer techniques. Low-sensitive methods, however, require cracks of higher strength, a strenuous task which requires a well-trained whip cracker. Problem (2) relates to the difficulty of sharply imaging the whip-lash as well as the shock which can only be done by an optical system with a large depth of focus and field of view. Problem (3) is the most difficult one, particularly if the shock emission is to be traced back in time to its local origin. This requires a special camera with pre-trigger framing, i.e. a camera which is permanently recording, but stopped by the occurrence of the crack itself, for example by an acoustical trigger. In addition, to perform the experiments economically, a recording technique with an immediate playback facility is essential.

4.2 Direct shadowgraphy

To fully visualize the whole mechanism of whip cracking, a large field of view of at least 2×8 m^2 would be required. Most of this area would be allotted to the initial phase in order to cover the movements of the operator and the development and propagation of the loop along the long whip-lash. The visualization of shock emission, however, is limited to a small field close to the whip-tip. Therefore, to resolve this supersonic phase in more detail, a selective enlargement is indispensable.

In order to visualize simultaneously the whip-tip dynamics and shock expansion an imaging system with a large depth of focus and a fairly large field of view are required. Shadowgraphy in parallel light would be ideal, but its field of view is limited to the diameter of available concave mirrors, normally not exceeding 60 cm. An alternative, although less sensitive, is the method of direct shadowgraphy, using a high-intensity point light source to cast a shadow of the object from a central projection. An intense light source is capable of illuminating a large field of view. The principal advantages of this technique are its simplicity and insensitivity to any heat or flow disturbances created by the movements of the whip operator. However, the shadowgraph technique is only capable of detecting strong changes in the index of refraction and is therefore only sensitive to strong cracks.

The experimental setup is shown schematically in Fig. 5. The light from an intense pulsed laser is focused onto a pin-hole with a diameter of 0.5 mm which acts as a point light source, evenly illuminating the screen. The objective lens of the high-speed framing camera is positioned as close as possible to the pin-hole and is focused on the screen via

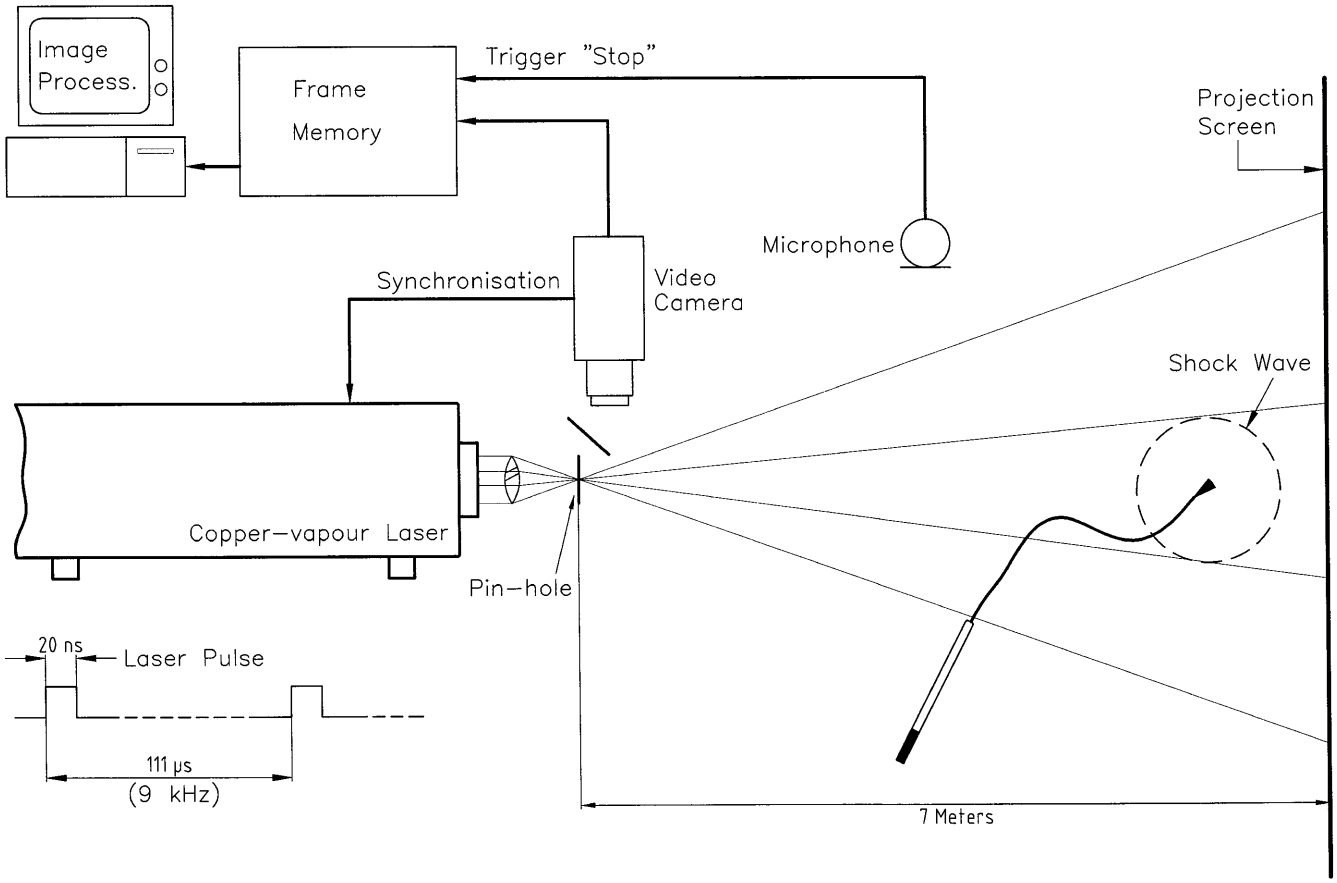

Fig. 5. Experimental setup for simultaneous recording of whip-tip motion and shock wave emission

a small mirror or prism. To absorb the scattered laser light from the camera objective it is helpful to use a small shield between camera and pin-hole.

When the whip-lash passes between the pin-hole and the screen with supersonic speed, it cast shadows of the whip lash and the disturbance caused by the shock front. Both are imaged by the camera side-inverted. The camera also records the whip-lash in front-light. In the arrangement of Fig. 5 the camera views the object under almost the same visual angle as its shadow, although both are positioned in different planes and the shadow image is larger than the object itself. This is an important advantage, because in practice it would be difficult to measure the actual distance between whip lash and screen in order to trace back the enlarged shadow image to its real dimensions. However, since there is an unavoidable small displacement between the pin-hole and the camera objective, the image taken in reflected light does not completely superimpose with its shadow image, cf. for example the image of the whip lash in Fig. 7. This small defect could be eliminated by, for example, using a beam-splitter. Disadvantageously, however, such a setup would reflect only a fraction of the light emerging from the screen. Furthermore, any scattering of the incident laser light at the beamsplitter would be detrimental to the image quality.

The optical resolution of the system is inversely related to the diameter of the pin-hole; directly related to the distance between pin-hole and screen, and inversely related to the distance between object or disturbance and screen (Schardin 1942, Hyzer 1962). The sensitivity depends on the strength of the crack and the distance between pin-hole and screen. In practice, a minimum distance is also required for the whip operator to provide sufficient clear room for his action. A good compromise between sensitivity and resolution is a position 1 m from the screen.

The screen used was a simple projection screen as commonly used for slide projection. A retro-reflective screen (Scotchlite) has a much higher reflectivity and, therefore needs a less intense light source (Edgerton 1979). However, a screen of the required size would need to be assembled from strips, and the resulting joint lines would impair the image quality.

4.3 Camera system

A Kodak EktaPro HS 4540 high-speed video recording system was used. At present this is the fastest video system commercially available. The standard video camera incorporates a dynamic digital memory which stores 1024 full frames at 4.5 kHz, each with up to 256 gray levels. This “resolving” buffer continually replaces old frames with new ones and can capture events which happened before the shock had reached the microphone (pre-trigger framing). The camera was stopped at a pre/post-event trigger ratio of 50%. The trigger signal was provided by a microphone closely positioned to the screen. The digital images could be replayed from the memory instantly. This permitted the forming and

analysis of a large number of cracks in a short time and facilitates the experiments considerably, because even for a trained whip operator it was not easy every time to place the whip-tip in its final motion within a field of view of only 1.2×0.6 m^2. The positions of the cracker and the shock wave were measured by displaying the digital images on a PC, counting the number of pixels and comparing them with a calibrated distance.

The maximum frame frequency of the camera was 40.5 kHz, but the CCD-matrix was then reduced to 64×64 pixels which was not sufficient to resolve the shock wave. A good compromise was to operate the camera in half-frame mode at 9 kHz, corresponding to an interframe time of 111 μs. The resulting 2:1 image format was also well adapted to the extended geometry of the whip-lash. The CCD sensor of the camera has a format of 10.24×10.24 mm^2 and in the half-frame mode uses 256(H) $\times$ 128(V) pixels. The pixel size of 40×40 μm^2 corresponds to an area of 4.7×4.7 mm^2 on the screen. For example, the shadow of a shock wave propagating with a Mach number of 2, cast on the screen and imaged onto the sensor surface, needs about 7 μs to propagate from one pixel to the next. Although the resulting spatial and temporal resolution are rather low, the image quality was still sufficient to resolve the supersonic phase and to trace the position of the shock front.

4.4 Pulsed light source

The high-intensity pulsed light source was a 25 W copper-vapour laser from Oxford Lasers, model ACL 25. The pulsed laser could be operated at a repetition frequency of up to 20 kHz. The duration of each pulse was in the order of 20 ns which provided an excellent stop motion capability. The laser was synchronized by the high-speed video camera system which could be operated only at various fixed recording rates. In the present case the camera was always operated in half-frame mode at 9 kHz.

Each laser pulse had a peak power of up to 200 kW, but a relatively high beam divergence of 6 mrad. Thus, only a fraction of the energy of each pulse passed through the pinhole. A standard laser system equipped with a plane-plane cavity was used. A better collimation at higher focusable power can be obtained by using an "off-axis" unstable cavity or an injection controlled oscillator/amplifier arrangement (Oxford Lasers 1988). In particular, the last mode results in a higher focusable power than provided by a plane-plane cavity to several orders of magnitude. This improvement would allow the use of lasers with a lower average power to illuminate a larger screen.

4.5 Whip construction

The whip illustrated in Fig. 1 was also used in our experiments. The stick had a length of 1.4 m and the thong a total length of 3.2 m and a total weight of 97 g. The lash parts (4)-(6) were made of a highly supple braided cord, consisting of hundreds of 20 μm thick polyamide (nylon) fibers. The cord had a specific weight of 3.75 g/m, an outer diameter of 2.5 mm and a rupture limit of 1100 N. The weight of the cracker including the knot amounted to 0.37 g. The terminal lash (6) had a total length of 0.6 m.

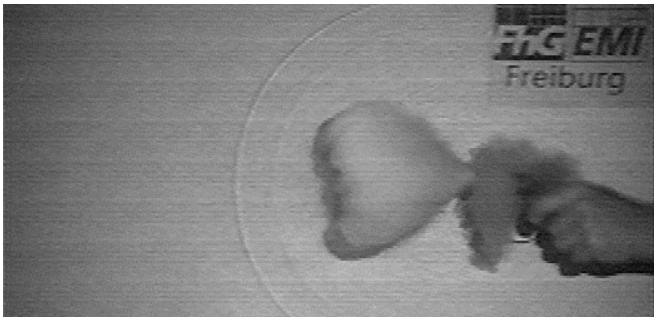

Fig. 6. Shock emission from a booby pistol

5 Results and conclusions

5.1 Sensitivity test

In order to test the sensitivity of the optical setup, we first visualized the shock emerging from a booby pistol which was fired parallel to the screen at a distance of about 1 m. We used blank cartridges with a caliber of 9×17 mm loaded with black powder (Dynamit Nobel # 380/9). Figure 6 has been selected from a series taken at a frame rate of 9 kHz. Close to the muzzle exit the blast wave has a velocity of more than 800 m/s which in a distance of 0.9 m reduces to about 600 m/s. The sensitivity test proved the method to be capable of clearly tracing the shock wave within the total area of the screen. However, for reproduction purposes the contrast in Figs. 6 and 7 has been slightly enhanced by image processing.

5.2 Whip-tip trajectory

The lash moved within the field of view for a time period of about 7 ms, corresponding to about 70 digital frames when operating at a frame rate of 9 kHz. Figure 7 shows some selected frames of such a series and illustrates the transition from the subsonic phase of whip-tip motion (cf. Fig. 7a) into the supersonic phase (cf. Fig. 7b–e) and the reversion into a subsonic phase (cf. Fig. 7f).

A complete series of digital frames allows a fairly good reconstruction of the trajectory of the whip-tip as shown in Fig. 8a. The trajectory shows whip-tip loci at equal time intervals and is a direct plot of experimental data obtained by the analysis procedure described in Sect. 4.3. Entering the supersonic phase of whip cracking at point B, the whip-tip loci increasingly stretch out and reach a maximum distance at point C, indicating that the tip has here reached its maximum velocity.

All theoretical models (Grammel and Zoller 1949, Szabó 1966, Bürger 1995) assume a motion of the whip-tip parallel to the straight part of the lash between stick and loop, as illustrated in Fig. 4. This assumption, however, which would result in a straight trajectory of the whip-tip, is not realistic, as shown in Fig. 8a. The curved nature of the trajectory is caused primarily by centrifugal forces rather than by a

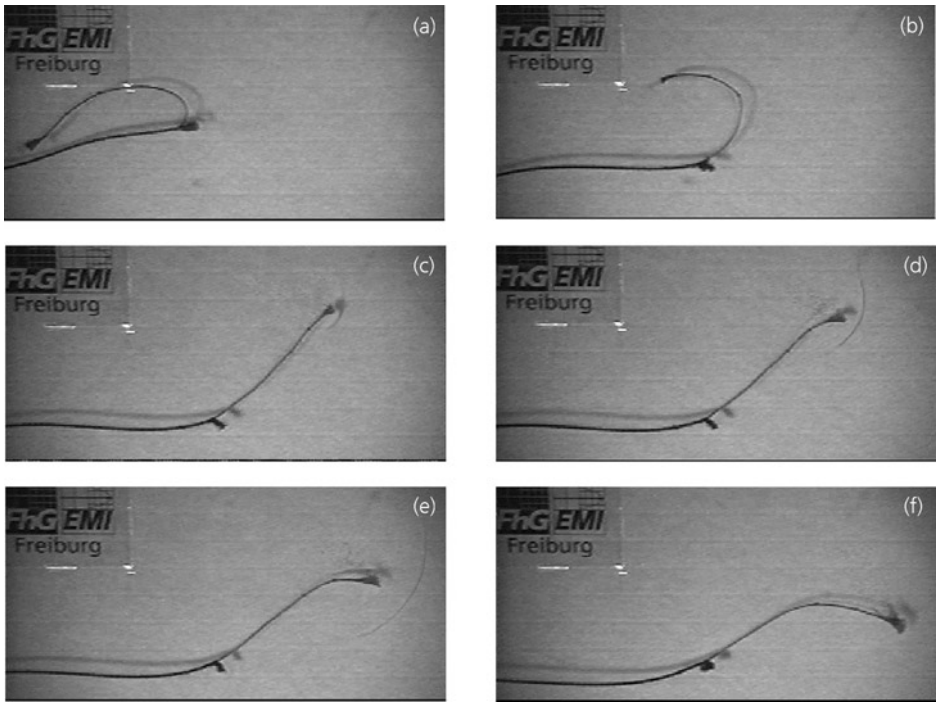

Fig. 7a–f. Cinematography of whip-tip motion at various Mach numbers and correlated shock wave emission: **a** subsonic phase, M = 0.69; **b** transonic phase, M = 0.85; **c** moment of maximum whip-tip velocity, M = 2.19; **d** during strong deceleration within the supersonic phase, M = 1.42; **e** shortly before leaving the supersonic phase, M = 1.29; and **f** back again in the subsonic phase, M = 0.6. Note that each frame is also superimposed by a faint ghost image of the preceding frame, a defect caused by the video camera at high frame rate

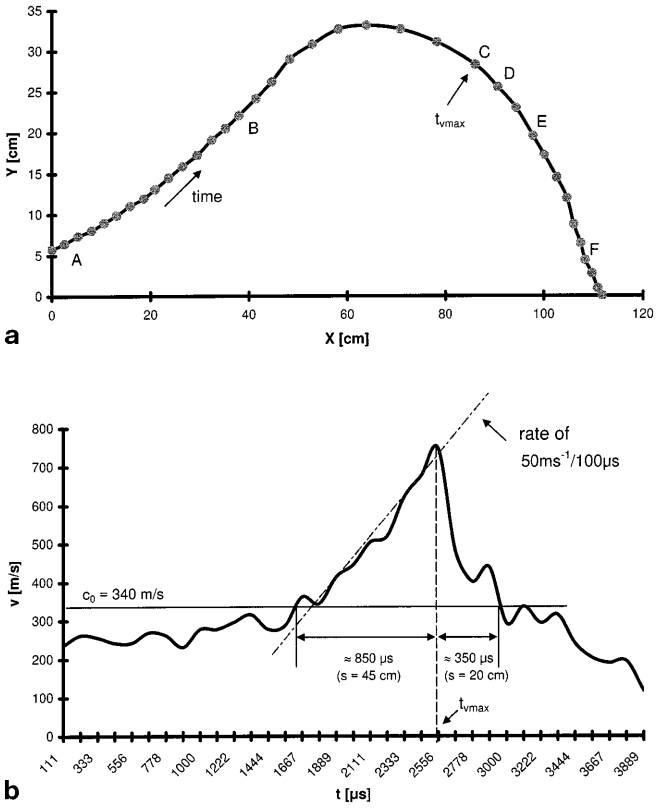

Fig. 8a,b. Whip-tip kinematics: **a** trajectory of the whip-tip, and **b** derived velocity of the whip-tip as a function of time. The points A...F marked in **a** relate to time instants shown in Figs. 7a–f

limited flexibility of the lash which in the present example was made of a highly flexible braid.

5.3 Velocity of the whip-tip

The resulting velocity v of the whip-tip along its trajectory is given by

$$v = \frac{\sqrt{\Delta x^2 + \Delta y^2}}{\Delta t},$$

where Δx and Δy are the changes in position at time step Δt and derived from neighboring experimental points shown in Fig. 8a. The velocity-time-profile of the whip-tip thus calculated results in a polygon. Figure 8b is a polynomial fit to the polygon data, obtained using *Microsoft Excel*. The most interesting phase, the supersonic phase of whip-tip motion, amounts to about 1300 μs and at the frame rate of 9 kHz was covered by 12 frames. The tuft at the whip-tip was accelerated within a distance of about 45 cm from a Mach number of M = 1 to a maximum of M = 2.19.

5.4 Shock wave emission

In Fig. 7c, the shock wave is seen for the first time at the moment when the whip-tip had reached its highest velocity. However, at that time the shock had already traveled some distance. Since the shadowgraph technique was not sensitive enough to resolve the steepening process, it is not possible to fully trace the shock wave back to its origin. A better temporal and spatial resolution would be desirable. A higher temporal resolution would be possible only by operating the camera at 18 kHz in the quarter-frame mode using a matrix of 256(H) $\times$ 64(V) pixels. However, in order to fully catch the supersonic phase of whip cracking it would be extremely difficult to place the whip-tip within the narrow field of view of only 1.2×0.3 m^2. The spatial resolution of video cameras is also rather low and still far beyond the minimum resolving power of 20 lp/mm obtainable on film.

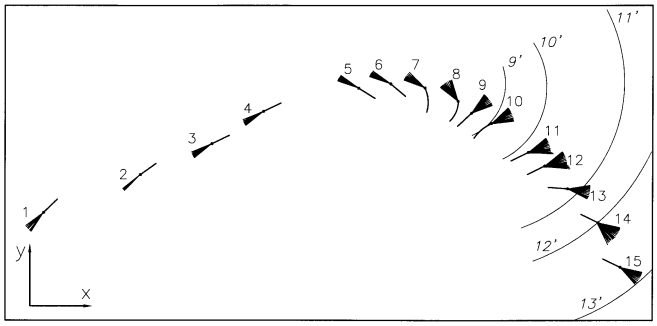

Fig. 9. Schematic sequence of temporal cracker positions $1 \rightarrow 15$ and corresponding shock wave positions $9' \rightarrow 13'$, illustrating the turning and unfolding mechanism of the tuft and the corresponding shock wave propagation. Note that for the sake of clarity the cracker and shock wave positions are not shown in equal time steps. Phases of cracker motion: subsonic $1 \rightarrow 3$; supersonic $4 \rightarrow 11$, and again subsonic $12 \rightarrow 15$. At position 9 the cracker has reached its maximum velocity (cf. also Fig. 7c), and the emitted shock wave at position $9'$ becomes visible for the first time

In the supersonic phase the whip-tip covered a distance of about 65 cm and moved in a highly non-steady mode, cf. Fig. 8b. Therefore, the head wave did not develop the well-known cone-shaped front as in the usual case of a steadily moving projectile (Mach and Salcher 1887). In the acceleration phase the maximum velocity of 744 m/s was reached after about 850 μs. In the shorter deceleration phase, lasting about 350 μs, the head wave has a parabolic-shaped geometry as in the case of a strongly decelerated projectile (Prandtl 1937). In this case the moving body (cracker) is increasingly lagging behind the shock front. Since the cracker was not moving on a straight line, the head wave was not exactly symmetrical. However, any shock focusing effects (Gobrecht 1970) resulting from this asymmetry could not develop because of the very short duration of the supersonic phase.

5.5 Behavior of the cracker

To generate a strong crack, it is very important that the cracker have a soft and dense tuft. The aerodynamic mechanism of the cracker is not yet fully understood. It is well-known that the drag coefficient of many bodies and projectiles of basic geometry, moving steadily and head-on along a straight trajectory, increases significantly within the transonic regime (cf. for example Dubs 1961). Corresponding data for a strongly accelerated motion along a curved trajectory do not exist. In addition, under these extreme conditions the aerodynamic behavior of fluffy bodies, such as the tuft of a cracker, has not yet been studied, which makes it very difficult to evaluate the aerodynamic behavior of the cracker in terms of transiently acting drag forces. However, a careful analysis of the series of experiments has clearly indicated that the mechanism of shock generation is primarily determined by the growing transverse position of the cracker when approaching the turning point of the whip-lash. Figure 9 schematically shows the increasing rotation of the cracker before, during and after passage of the supersonic phase which amounts in total to more than 250°.

At a low velocity of about 200 m/s the cracker still moves horizontally head-on with the tuft only a little opened. This may be caused by drag forces acting along the tuft fibers, cf. Fig. 7a and Fig. 9 at position 1. Subsequently, increasing in speed and entering the transonic regime, the tuft fibers close tightly and take on the diameter of the lash, cf. Fig. 7b and Fig. 9 at position 2. Starting at position 4, the cracker moves with supersonic velocity and at position 8 approaches the turning point which is not a sharp discontinuity, but has a radius of about 9 cm. The centrifugal forces, acting now increasingly onto the tuft, are larger at the free end than at the knot side and promote a sudden, pendulum-like revolution of the tuft fibers round the knot by almost 90°, cf. positions $8 \rightarrow 9$. The cracker reaches its maximum velocity at position 9, cf. also Fig. 7c. This process of turning over, occurring in a short time interval of about 100 μs, generates a strong volume flow, thereby transforming the stored kinetic energy very effectively into an acoustic shock. In the subsequent phase of extreme deceleration, the fibers spread apart as shown at positions $13 \rightarrow 15$, remniscent of the unfolding of an umbrella.

The shadowgraph method, capable only of resolving strong shocks, does not show any shock emission from the tuft within positions $4 \rightarrow 8$, although already moving with supersonic velocity. This leads to the important conclusion that for generating strong shocks the supersonic motion of the tuft is only a *conditio sine qua non*, but that the essential mechanism is the abrupt turning of the tuft in the final stage of acceleration.

As shown in Fig. 8b the velocity of the cracker steadily increases in the acceleration phase with a remarkable rate of 50 m/s per 100 μs, corresponding to an acceleration of 50,000 g. This momentarily produces an extreme tension in the lash and provokes a heavy wear and tear of the tuft fibers which need frequent trimming. The very high transient tension loading of the fibers may also explain the emission of micro projectiles from a lash made of a braided copper wire, as mentioned in Sect. 2. The absolute value of the deceleration even surpasses the maximum acceleration. Since the weight of the cracker is small, but the area exposed and, therefore, the provoked drag force, are quite large, the deceleration process from $M > 2$ back to $M < 1$ occurs within a surprisingly short distance of only 20 centimeters.

Acknowledgements. The authors are grateful for discussions with Prof. Dr. W. Bürger from the Institute of Theoretical Mechanics of the University of Karlsruhe and with Dr. G. Smeets and his colleagues from the German-French Research Institute (ISL), Saint Louis, France. Thanks are also due to P. Müller and R. Weiß from the *Höllenzunft Kirchzarten*, Black Forest, for providing the whip cracking.

References

Bernstein B, Hall DA, Trent HM (1958) On the Dynamics of a Bull Whip. JASA 30:1112

Boys CV(1893) On electric spark photographs; or photography of flying bullets etc. by the light of the electric spark. Nature 47:415 and 440

Bürger W (1995) Peitschenknall mit Überschall. Bild der Wissenschaft, Heft 8, pp 102-103

Carrière Z (1927) Le claquement du fouet. J. de Physique et Le Radium Ser. VI, 8:365

Carrière Z (1955) Exploration par le fouet des deux faces du mur du son. Cahiers de Physique No. 63, pp 1–17

Dubs F (1961) Hochgeschwindigkeitsaerodynamik. Birkhäuser, Basel and Stuttgart, pp 120–121

Edgerton HE (1979) Electronic Flash, Strobe. MIT Press, Cambridge, MA, and London, 2nd ed., pp 343–344

Glass II (1974) Shock Waves and Man. University of Toronto Press, pp 31–33

Gobrecht H (1970) Lehrbuch der Experimentalphysik. Band 1: Mechanik, Akustik, Wärme. De Gruyter, Berlin, p 496

Grammel R, Zoller K (1949) Zur Mechanik des Peitschenknalles. Z. Physik, 127:11

Hyzer WG (1962) Engineering and Scientific High-Speed Photography. Macmillan, New York, p 426

Kapfhammer G (ed.) Brauchtum in den Alpenländern. Callwey-Verlag, Munich

Kucharski W (1941) Zur Kinetik dehnungsloser Seile mit Knickstellen. Ing.-Arch. 12:109

Lummer O (1905) Über die Theorie des Knalls. Schlesische Gesellschaft für vaterländische Kultur 83,II:2

Mach E, B. Doss (1893) Bemerkungen zu den Theorien der Schallphänomene bei Meteoritenfällen. Sitzungsber. Akad. Wiss. Wien (II. Abth.) 102:248

Mach E, Salcher P (1887) Photographische Fixierung der durch Projectile in der Luft eingeleiteten Vorgänge. Sitzungsber. Akad. Wiss. Wien (II. Abth.) 95:764

Mezger, W (1997) Institut für Volkskunde der Universität Freiburg. Private communication

Mezger, W (1991) Narrenidee und Fasnachtsbrauch - Studien zum Fortleben des Mittelalters in der europäischen Festkultur. Habilitationsschrift Universität Freiburg, Universitätsverlag Konstanz

Oxford Lasers Ltd, Oxford, OX4 1RD, U.K.. Cavity designs for metal vapour lasers. Technical Note No.1 (1988)

Prandtl L (1913) Gasbewegung. Handwörterbuch der Naturwissenschaften 4:544, Fischer, Jena

Prandtl L (1937) Über Schallausbreitung bei rasch bewegten Körpern. Schriften der Deutschen Akademie der Luftfahrtforschung, Heft 7, 14 pages

Schardin H (1942) Die Schlierenverfahren und ihre Anwendungen. Ergebn. exakten Naturwiss. 20:303

Szabó I (1966) Einführung in die Technische Mechanik. Springer, Berlin, Heidelberg, and New York, 7th ed., pp 331–334

Szabó I (1972) Repertorium und Übungsbuch der Technischen Mechanik. Springer, Berlin, Heidelberg, and New York, 3rd ed., pp 176–178

Szabó I (1972) Höhere Technische Mechanik. Springer, Berlin, Heidelberg, and New York, 5th ed., pp 131–132

Winkelmann A, editor (1909) Handbuch der Physik. 2. Band: Akustik. Barth, Leipzig, 2nd ed., pp 437–523